

**Sources, fluxes, and behaviors of fluorescent dissolved organic matter (FDOM) in the  
Nakdong-River Estuary, Korea**

Shin-Ah Lee<sup>1</sup> and Guebuem Kim<sup>1\*</sup>

<sup>1</sup>School of Earth and Environmental Sciences/Research Institute of Oceanography, Seoul  
National University, Seoul 08826, Republic of Korea

\*Corresponding author. Tel : +82-2-880-7508; Fax : +82-2-876-6508

E-mail address: gkim@snu.ac.kr (G.Kim)

Submitted to *Biogeosciences* (Revised version)

## Abstract

We monitored seasonal variations of dissolved organic carbon (DOC), stable carbon isotope of DOC ( $\delta^{13}\text{C}$ -DOC), and fluorescent dissolved organic matter (FDOM) in water samples from a fixed station in the Nakdong-River Estuary, Korea. Sampling was performed every hour during spring tide once a month from October 2014 to August 2015. The concentrations of DOC and humic-like FDOM showed significant negative correlations against salinity ( $r^2=0.42-0.98$ ,  $p < 0.0001$ ), indicating that the river-originated DOM components are the major source and behave conservatively in the estuarine mixing zone. The extrapolated  $\delta^{13}\text{C}$ -DOC values ( $-27.5 - 24.5\%$ ) in fresh water confirm that both components are mainly of terrestrial origin. The slopes of humic-like FDOM against salinity were 60-80% higher in the summer and fall, due to higher terrestrial production of humic-like FDOM. The slopes of protein-like FDOM against salinity, however, were 70-80% higher in spring, due to higher biological production in river water. Our results suggest that there are large seasonal changes in riverine fluxes of humic and protein-like FDOM to the ocean.

## 1. Introduction

The global annual flux of dissolved organic carbon (DOC) via rivers is approximately  $0.17 - 0.36 \times 10^{15}$  g (Meybeck, 1982; Ludwig et al., 1996; Dai et al., 2012). The DOC delivered from riverine discharges as well as *in situ* production through biological activities significantly affects carbon and biogeochemical cycles in coastal waters (Hedges, 1992; Bianchi et al., 2004; Bauer et al., 2013; Moyer et al., 2015).

Generally, DOC includes fluorescent dissolved organic matter (FDOM), which emits fluorescent light due to its chemical characteristics. As FDOM accounts for 20 - 70% of the DOC in coastal waters (Coble, 2007) and controls the penetration of harmful UV radiation in the euphotic zone, it plays a critical role in carbon cycles as well as biological production. In addition, FDOM is known as a powerful indicator of humic and protein-like substances (Coble, 2007) in coastal waters. River discharge is generally the main source of humic-like FDOM in coastal waters, although it is also produced through *in situ* microbial activity (Romera-Castillo et al., 2011). In contrast, protein-like FDOM is known to be from biological production as well as anthropogenic sources (Baker and Spencer, 2004). Terrestrial humic substances behave conservatively in coastal areas due to their refractory characteristics (Del Castillo et al., 2000), whereas protein substances behave non-conservatively in many estuaries due to their relatively rapid production and degradation (Vignudelli et al., 2004).

The magnitudes of DOC and FDOM fluxes from rivers are generally dependent on rainfall, discharge, and temperatures (Maie et al., 2006; Jaffé et al., 2004; Huang and Chen,

2009). In the estuarine mixing zone, intensive biogeochemical processes occur through photo-oxidation, microbial degradation, or physicochemical transformations (i.e., flocculation, sedimentation) (Bauer and Bianchi, 2011; Moran et al., 1991; Benner and Opsahl, 2001; Raymond and Bauer, 2001). Recent studies have demonstrated large seasonal variations as high as 40%, in DOC export from rivers to the ocean (Burns et al., 2008; Bianchi et al., 2004; Dai et al., 2012). However, the seasonal variations in sources, fluxes, and behaviors of DOC and FDOM in the estuarine mixing zone are still poorly understood.

In this study, we analyzed DOC,  $\delta^{13}\text{C}$ -DOC, and FDOM in estuarine water samples collected monthly from the Nakdong-River estuary. Sampling was conducted at a fixed platform, which has been utilized for monitoring various environmental parameters. This sampling station is advantageous because we can collect water samples for a wide range of salinities throughout tidal fluctuations. Using the data obtained from this unique station, we were able to determine (1) the behaviors of DOM in the estuarine mixing zone, (2) the fluxes of DOM from rivers based on the slopes between salinities and DOM components, and (3) the changes in DOM sources using  $\delta^{13}\text{C}$ -DOC in the estuarine samples. The slope measurement in the mixing zone may represent the endmember of DOM components in rivers better than site-specific measurements in the river, by integrating larger spaces and times.

## **2. Materials and methods**

### *2.1 Study site*

The Nakdong-River Estuary, which is the estuary of the longest river in Korea, is a

major source of water supplying the needs for drinking, agriculture, and industry. The main channel of Nakdong River is approximately 510 km in length with a watershed area of approximately 23,380 km<sup>2</sup>. It faces the south-eastern coastal area of the Korean peninsula, passing through Busan which is the second largest city in Korea. The mean annual precipitation is 1150 mm, and most precipitation (60-70%) occurs during the summer monsoon and typhoon seasons (Jeong et al., 2007). To manage water supply and saltwater intrusion, estuary dams were constructed in the mouth of the river in 1987.

## *2.2 Sampling*

Water samples were collected at the sampling site which is located 560 m downstream from the dam (Fig. 1). The sampling period was from October 2014 to August 2015. The 2-L water sampling was conducted every hour for 24 hours during spring tide using an auto-sampler (RoboChem<sup>TM</sup>Autosampler, Model S3-1224N, Centennial Technology, Korea), with a depth of the water intake 1 m below the surface. After samples were collected in acid-cleaned polyethylene bottles, they were moved to the laboratory within 24 hours. All water samples were filtered using pre-combusted GF/F filters. The FDOM samples were stored in pre-combusted amber glass vials and kept below 4°C in a refrigerator before analysis. The DOC and  $\delta^{13}\text{C}$ -DOC samples were acidified to pH ~2 using 6 M HCl to avoid bacterial activities and stored in pre-combusted glass ampoules. Ampoules were fire-sealed to prevent the samples from any contaminations. The samples were analyzed for DOC and CDOM within a week. Salinity was measured using a YSI Pro Series conductivity probe sensor in the laboratory. The real-time and compulsory discharge volume data from the dam are available at <http://www.water.or.kr>, provided by K-Water. The monitoring program at this station is

maintained by Korea Environment Management Corporation (KOEM). The water temperature data are recorded automatically at the site. The data are available at <https://www.koem.or.kr>.

### *2.3 Analytical methods*

The concentrations of DOC were determined by a high-temperature catalytic oxidation (HTCO) method using a TOC-VCPH analyzer (Shimadzu, Japan). Standardization was performed based on the calibration curve of acetanilide in ultra-pure water. The acidified samples were purged with carbon dioxide (CO<sub>2</sub>) free carrier gas for 2 min to remove inorganic carbon. The samples were then injected into a combustion column packed with Pt-coated alumina beads and heated to 720°C. The CO<sub>2</sub> evolving from combusted organic carbon was detected by a non-dispersive infrared detector (NDIR). Our DOC method was verified with Deep Seawater Reference (DSR) samples for DOC (44-46 µmol L<sup>-1</sup>) produced by the University of Miami, USA.

The values of δ<sup>13</sup>C-DOC were measured using a TOC-IR-MS instrument consisting of an IR-MS instrument coupled with a Vario TOC cube (Isoprime, Elementar, Germany). The TOC instrument uses a common high-temperature catalytic combustion method (Kirkels et al., 2014). The analytical method is fully described in Kim et al. (2015). Briefly, 10 mL of filtered samples was purged with O<sub>2</sub> gas for 20–30 min to completely remove DIC after the samples were acidified to pH ~2. Then, 1 mL of the sample was injected into Pt-impregnated catalyst in a quartz tube. In this tube, the DOC was converted completely to CO<sub>2</sub> at 750°C, which was then fed through a water trap followed by a halogen trap. After DOC was detected by an NDIR

detector, the CO<sub>2</sub> gas was entered the TOC–IR–MS interface by the O<sub>2</sub> carrier gas. In the interface, the CO<sub>2</sub> was transferred to the IR–MS instrument following the removal of any interfering gasses. The δ<sup>13</sup>C-DOC value of blank was measured using the Low Carbon Water (LCW) from Hansell lab (University of Miami), which contains less than 2 μM DOC. Certified IAEA-CH6 sucrose (International Atomic Energy Agency,  $-10.45 \pm 0.03\%$ ) prepared with the low carbon water was used as a standard solution. A standard sample was analyzed for every sample queue (once before or after ten samples) to check a drifting effect during the measurements. The blank correction was performed using a method previously described in De Troyer et al. (2010) and Panetta et al. (2008). Our measurement result of δ<sup>13</sup>C-DOC for the DSR (University of Miami) was  $-21.5 \pm 0.1\%$ , which is consistent with the results reported by Panetta et al. (2008) and Lang et al. (2007). The reproducibility of TOC–IR–MS was ~0.3%.

FDOM fluorescence was determined in a scan mode using a spectrofluorometer (SCINCO FluoroMate FS-2) within two days after sampling. Emission (Em) spectra were collected from 250 to 600 nm at 2 nm intervals at excitation (Ex) wavelengths from 250 nm to 500 nm at 5 nm intervals. Backgrounds were subtracted for fresh distilled water prepared daily from the sample data to eliminate Raman Scatter peaks (Zepp et al., 2004). All data were obtained in counts per second (cps) and converted to a ppb quinine sulfate standard solution in 0.1 N sulfuric acid at Ex/Em of 350/450 nm. The inner filter effect was negligible for these estuarine water samples using this instrument since the correlation between the uncorrected and corrected values for the inner filter effect was very significant for some samples ( $r^2=1$ ,  $n=5$ ). EEMs-PARAFAC analysis was performed using a MATLAB R2013a program with a DOMFluor toolbox.

### 3. Results and Discussion

Salinities ranged from 0.1 to 28.5 over the sampling period of a year. Salinities in the sampling location were dependent primarily on the volume of river-water discharge from the dam. The volumes of river discharge were relatively larger in October, April, July, and May. The mean annual surface water temperature was 16°C, with the lowest temperature (avg. 8°C) in December and the highest temperature in August (avg. 26°C).

#### *3.1 Behaviors and sources of DOC in the estuarine mixing zone*

The concentrations of DOC ranged from 100 to 300 µM, with the highest concentrations in July (avg. 243 µM) and the lowest concentrations in February (avg. 115 µM), consistent with the typical DOC concentration ranges in coastal waters (Wang et al., 2004; Raymond and Bauer, 2001). The concentrations of DOC correlated significantly with salinities ( $r^2 = 0.59-0.92$ ,  $p < 0.0001$ ), indicating that DOC behaves conservatively in the mixing zone of this estuary (Fig. 2A), which is commonly observed in estuarine mixing zones (Laane, 1980; Mantoura and Woodward, 1983; Del Castillo et al., 2000; Clark et al., 2002; Jaffé et al., 2004).

If the high salinity periods are excluded, both the slope and y-intercept of DOC concentrations versus salinities were highest in July (Fig. 1), which could be due to a higher terrestrial DOC loading in the summer period, as observed in Horsens Fjord, Denmark (Markager et al., 2011). For this comparison, we excluded the high-salinity periods ( $>20$ ), including December, January, February, and June, since they showed a narrow and low DOC



concentration range (103-163  $\mu\text{M}$ ), resulting in large uncertainties by extrapolating them to the fresh water.

The carbon isotope values in the Nakdong-River Estuary ranged from -28.2 ‰ to -17.6. In order to determine the source of DOC in fresh water, we plotted  $\delta^{13}\text{C}$ -DOC values against salinities (Fig. 2B). The conservative mixing curve of  $\delta^{13}\text{C}$  values can be obtained using the two endmember mixing equation (Spiker, 1980; Raymond and Bauer, 2001):

$$\delta^{13}\text{C}_s = \frac{F_r \delta^{13}\text{C}_r [\text{DOC}]_r + (1-F_r) \delta^{13}\text{C}_m [\text{DOC}]_m}{[\text{DOC}]_s} \quad (1)$$

where  $\delta^{13}\text{C}_s$ ,  $\delta^{13}\text{C}_r$  and  $\delta^{13}\text{C}_m$  are the  $\delta^{13}\text{C}$ -DOC values at a given sample salinity, river endmember salinity, and marine endmember salinity, respectively;  $F_r$  is the riverine freshwater fraction calculated from the measured salinities;  $[\text{DOC}]_s$  and  $[\text{DOC}]_m$  are the DOC concentrations at a given salinity and marine endmember salinity, respectively;  $[\text{DOC}]_r$  is the endmember DOC value for the river water (Fig. 1).

The riverine DOC endmember values ( $S=0\text{‰}$ ) ranged from 174 to 284  $\mu\text{M}$ . The marine endmember value ( $S=29\text{‰}$ ) of DOC is 100  $\mu\text{M}$  with the  $\delta^{13}\text{C}$ -DOC value of -19‰. If these values from each month are applied, the  $\delta^{13}\text{C}$ -DOC endmember values for the river water extrapolated to be from -27.5 to -24.5‰ (average: -26.2‰). Overall, the carbon isotope values of our samples are fitted well into the conservative mixing curve of the overall trend, with a slight change using different endmember values for different months (Fig. 2B). In general,  $\delta^{13}\text{C}$ -DOC values range from -22 to -18‰ for marine phytoplankton, from -34‰ to -23‰ for terrestrial C3 plants, and from -16‰ to -10‰ for terrestrial C4 plants (Gearing 1988; Clark

and Fritz, 1997). Carbon isotope values in our study confirm that the main source of DOC in the estuarine mixing zone is dominantly from terrestrial C3 plants over all seasons. However, the value was heavier at lower salinity ranges ( $S < 10$ ) in March and April samples, perhaps in association with the higher biological production in the river.

### *3.2 Behaviors and sources of FDOM in the estuarine mixing zone*

Four components were identified in the water samples from the EEMs dataset. Based on the excitation-emission peak location, Component 1 (FDOM<sub>H</sub>, Ex/Em = 320/418 nm) is found to be a terrestrial humic-like component (C peak) shown by Coble (2007). Component 2 (FDOM<sub>P</sub>, Ex/Em = 280/328 nm) is found to be a tryptophan-like component (T peak), which is produced by microbial processes. Component 3 (Ex/Em = 300,325/364 nm) is found to be a marine humic-like component (M peak). Since Component 3 values were significantly correlated with Component 1 ( $r^2=0.95$ ) values, we simply focused on Component 1 (FDOM<sub>H</sub>) and Component 2 (FDOM<sub>P</sub>) for data interpretations.

The concentrations of FDOM<sub>H</sub> ranged from 2.4 to 19.7 quinine sulfate unit (QSU), with the highest concentration in July (avg. 17.6 QSU) and the lowest concentration in June (avg. 3.4 QSU) (Fig. 2C). The concentrations of FDOM<sub>P</sub> ranged from 0.6 to 22.4 QSU, with the highest concentration in March (avg. 15.1 QSU) followed by October (avg. 13.6 QSU) (Fig. 2D).

The concentrations of both FDOM components were significantly correlated with salinities ( $r^2 = 0.42-0.98$ ,  $p < 0.0001$  for FDOM<sub>H</sub> and  $r^2 = 0.27-0.96$ ,  $p < 0.0001$  for FDOM<sub>P</sub>), indicating that they are conservative in the mixing zone (Fig. 2). The slopes of FDOM<sub>H</sub> and FDOM<sub>P</sub> for each month ranged from -0.15 to -0.59 and -0.15 to -0.71, respectively. The higher FDOM<sub>H</sub> slopes in July and October were similar to the trend of DOC (Fig. 2C), which could be due to higher terrestrial FDOM production. However, the seasons (March and April) in which higher FDOM<sub>P</sub> slopes occurred differ from those of DOC and FDOM<sub>H</sub>, indicating that both FDOM components have different source inputs (Fig. 2D).

Although there are large differences in scattering of FDOM components against salinities, it is very difficult to compare scatterings for different seasons in order to discuss the different behaviors of DOM since the scattering is generally larger for the narrow salinity ranges. If the winter data are excluded, in March, during the highest biological production period in the river, the correlation coefficient against salinities was the highest for FDOM<sub>P</sub> and lowest for FDOM<sub>H</sub>. In contrast, in June, during the highest fluvial DOM discharge period, the correlation coefficient against salinities was the highest for FDOM<sub>H</sub> and lowest for FDOM<sub>P</sub>. This suggests that the biological production and removal, together with other generally known factors such as photo-degradation and sedimentary inputs, may affect the scattering of these FDOM components in the estuarine mixing zone.

As such, there was a significant positive correlation between FDOM<sub>H</sub> and DOC concentrations throughout all sampling periods ( $r^2 = 0.93$ ,  $p < 0.0001$ ) (Fig. 3A), suggesting that the main source of FDOM<sub>H</sub> and DOC is terrestrial based on  $\delta^{13}\text{C}$ -DOC values. Since FDOM

does not usually contribute to a major portion of DOC, a positive correlation between FDOM and DOC has only been observed in specific areas, such as river-estuarine systems (Del Vecchio and Blough, 2004; Coble, 2007). Stedmon et al., (2006) demonstrated that stronger correlations were observed between DOC and FDOM as humic substances derived from terrestrial DOM are more colored than DOM produced *in situ*. In general, terrestrial DOM occurring in rivers originates mainly from plant decomposition and leaf litter in the form of humic substances (Huang and Chen, 2009). As such, Gueguen et al., (2006) showed that humic materials are more effectively extracted from soils during August and September under high temperatures. Thus, higher FDOM<sub>H</sub> slopes in August, October, and November, relative to the other periods, could be associated with higher terrestrial inputs of degradation products of soil organic matter (Dowell, 1985; Qualls et al., 1991).

In the study region, FDOM<sub>P</sub> concentrations were poorly correlated with DOC concentrations ( $r^2=0.11$ ) (Fig. 3B). The slopes of FDOM<sub>P</sub> concentrations against DOC concentrations varied significantly over different seasons, with steeper gradients in the spring (March and April) and fall (October). In general, FDOM<sub>P</sub> is known to be produced efficiently by biological production in water (Coble, 1996; Belzile et al., 2002; Steinberg et al., 2004; Zhao et al., 2017). Thus, higher FDOM<sub>P</sub> concentrations, relative to DOC concentrations, in the spring and fall seems to be associated with the spring and fall phytoplankton blooms in river waters (Mayer et al., 1999; Zhang et al., 2009).

### 3.3 Fluxes of DOC and FDOM in the estuarine mixing zone

The fluxes of DOC and FDOM from rivers to the ocean are calculated using the endmember values (C) of these components in rivers multiplied by the river discharge volumes (Q) for each month (Fig. 4). For this estimation, we assumed that (1) the endmember values are the same as the intercepts of the DOC, FDOM<sub>H</sub>, and FDOM<sub>P</sub> versus salinity plots, and (2) the endmember values measured in the spring tides represent the concentrations of these components for each month.

River discharge was highest in April and July following heavy precipitation, and the largest discharge volume was about five-fold higher than that of winter discharges (Fig. 4A). However, the monthly variations of DOC endmember (y-intercept) values were quite constant, ranging from 174 - 284  $\mu\text{M}$ . This indicates that the concentrations of DOC in the river are independent of river discharge volumes (Fig. 4B). The DOC endmember values were highest in December, followed by July and June (Fig. 4B). The monthly variation trend of FDOM<sub>H</sub> endmember values was similar to that of DOC, except for the December value. Excluding the December values, the FDOM<sub>P</sub> endmember values were highest in March, February, and October. These endmember trends are consistent with the slope variations explained in the previous section. Although there are large uncertainties in fresh water endmember values of DOC and FDOM in winter owing to narrow, high salinity ranges, we used the endmember values for the flux comparisons since the contribution of the uncertainties may be relatively small due to smaller river discharge volumes in winter.

The riverine DOC flux ranged from  $1.6 \times 10^6 \text{ mol day}^{-1}$  (February) to  $12.3 \times 10^6 \text{ mol day}^{-1}$  (July), indicating that there are large variations of DOC fluxes to the ocean. The riverine

flux of  $\text{FDOM}_H$  and  $\text{FDOM}_P$  ranged from  $1.4 \times 10^9 \text{ QSU m}^3 \text{ day}^{-1}$  (December) to  $23.1 \times 10^9 \text{ QSU m}^3 \text{ day}^{-1}$  (July) and from  $1.6 \times 10^9 \text{ QSU m}^3 \text{ day}^{-1}$  (June) to  $16.4 \times 10^9 \text{ QSU m}^3 \text{ day}^{-1}$  (March), respectively. The seasonal variation trend of  $\text{FDOM}_H$  was similar to that of DOC. The fluxes of  $\text{FDOM}_P$  in December and March were twofold higher than those of  $\text{FDOM}_H$  whereas the flux of  $\text{FDOM}_H$  in July was 2-3 folds higher than that of  $\text{FDOM}_P$ . This shows that the fluxes of both components of FDOM differ significantly by seasons owing to the different source inputs even though their magnitudes are controlled mainly by river discharges

It is well known that the single sampling event is not enough to capture the full range of natural variability in DOM abundance over all seasons (Stedmon et al., 2006; Huang and Chen, 2009; Markager et al., 2011; Dai et al., 2012; Moyer et al., 2015). Overall, our results show that monthly variations are significant. This implies that our understanding of DOC fluxes from large rivers is largely biased, depending on sampling resolution, methods, and hydrogeological settings of a specific river. For example, if summer data are extrapolated to annual river water discharge, the DOC and  $\text{FDOM}_H$  fluxes can be overestimated up to three times for the Nakdong River.

#### **4. Conclusions**

The concentrations of  $\text{FDOM}_H$  and DOC showed significant negative correlations against salinities throughout all sampling periods, indicating that they behave conservatively in this estuarine mixing zone. The slopes of both DOC and  $\text{FDOM}_H$  concentrations versus salinities were highest in July, due to the largest terrestrial DOC loadings. The carbon isotope values showed that the main source of DOC in the estuarine mixing zone is terrestrial  $\text{C}_3$  plants

over all seasons. The slopes of FDOM<sub>P</sub> versus salinity were relatively higher in March and April in association with the spring phytoplankton blooms in river and estuarine waters. The monthly fluxes of DOC, FDOM<sub>H</sub>, and FDOM<sub>P</sub> showed large seasonal variations (5-10 folds), suggesting that the estimation of annual riverine fluxes of DOC, FDOM<sub>H</sub>, and FDOM<sub>P</sub> requires careful considerations of seasonal changes in rivers.

### **Competing interests**

The authors declare that they have no conflict of interest.

### **Acknowledgements**

We thank the Environmental and Marine Biogeochemistry Laboratory (EMBL) members for their assistance with sampling and laboratory analyses. This work was supported by the National Research Foundation of Korea (NRF) grant funded by the Korean government (MEST) (NRF-2015R1A2A1A10054309) and by the project titled "Deep Water Circulation and Material Cycling in the EAST Sea (2016)", funded by the Ministry of Oceans and Fisheries, Korea.

### **References**

- Baker, A., and Spencer, R. G.: Characterization of dissolved organic matter from source to sea using fluorescence and absorbance spectroscopy, *Sci. Total Environ.*, 333, 217-232, 2004.
- Bauer, J., and Bianchi, T.: 5.02—dissolved organic carbon cycling and transformation, *Treatise on estuarine and coastal science*. Academic Press, Waltham, 7-67, 2011.

325 Bauer, J. E., Cai, W.-J., Raymond, P. A., Bianchi, T. S., Hopkinson, C. S., and Regnier, P. A.:  
 326 The changing carbon cycle of the coastal ocean, *Nature*, 504, 61, 2013.

327 Belzile, C., Gibson, J. A., and Vincent, W. F.: Colored dissolved organic matter and dissolved  
 328 organic carbon exclusion from lake ice: Implications for irradiance transmission and carbon  
 329 cycling, *Limnol. Oceanogr.*, 47, 1283-1293, 2002.

330 Benner, R., and Opsahl, S.: Molecular indicators of the sources and transformations of  
 331 dissolved organic matter in the Mississippi river plume, *Org. Geochem.*, 32, 597-611, 2001.

332 Bianchi, T. S., Filley, T., Dria, K., and Hatcher, P. G.: Temporal variability in sources of  
 333 dissolved organic carbon in the lower Mississippi River, *Geochim. Cosmochim. Acta*, 68, 959-  
 334 967, 2004.

335 Burns, K. A., Brunskill, G., Brinkman, D., and Zagorskis, I.: Organic carbon and nutrient fluxes  
 336 to the coastal zone from the Sepik River outflow, *Cont. Shelf Res.*, 28, 283-301, 2008.

337 Clark, I.J., and Fritz, P.: *Environmental Isotopes in Hydrogeology*, CRC Press/Lewis Publishers,  
 338 Boca Raton, 1997.

339 Clark, C. D., Jimenez-Morais, J., Jones, G., Zanardi-Lamardo, E., Moore, C. A., and Zika, R.  
 340 G.: A time-resolved fluorescence study of dissolved organic matter in a riverine to marine  
 341 transition zone, *Mar. Chem.*, 78, 121-135, 2002.

342 Coble, P. G.: Characterization of marine and terrestrial DOM in seawater using excitation-  
 343 emission matrix spectroscopy, *Mar. Chem.*, 51, 325-346, 1996.

344 Coble, P. G.: Marine optical biogeochemistry: the chemistry of ocean color, *Chemical reviews*,  
 345 107, 402-418, 2007.



346 Dai, M., Yin, Z., Meng, F., Liu, Q., and Cai, W.-J.: Spatial distribution of riverine DOC inputs  
 347 to the ocean: an updated global synthesis, *Current Opinion in Environmental Sustainability*, 4,  
 348 170-178, <https://doi.org/10.1016/j.cosust.2012.03.003>, 2012.

349 De Troyer, I., Bouillon, S., Barker, S., Perry, C., Coorevits, K., and Merckx, R.: Stable isotope  
 350 analysis of dissolved organic carbon in soil solutions using a catalytic combustion total organic  
 351 carbon analyzer-isotope ratio mass spectrometer with a cryofocusing interface, *Rapid Commun.*  
 352 *Mass Spectrom.*, 24, 365-374, 2010.

353 Del Castillo, C. E., Gilbes, F., Coble, P. G., and Müller-Karger, F. E.: On the dispersal of  
 354 riverine colored dissolved organic matter over the West Florida Shelf, *Limnol. Oceanogr.*, 45,  
 355 1425-1432, 2000.

356 Del Vecchio, R., and Blough, N. V.: Spatial and seasonal distribution of chromophoric  
 357 dissolved organic matter and dissolved organic carbon in the Middle Atlantic Bight, *Mar.*  
 358 *Chem.*, 89, 169-187, 2004.

359 Dowell, W. H.: Kinetics and mechanisms of dissolved organic carbon retention in a headwater  
 360 stream, *Biogeochemistry*, 1, 329-352, 1985.

361 Gearing, J.N., The use of stable isotope ratios for tracing the nearshore–offshore exchange of  
 362 organic matter. In: Jansson, B.-O. (Ed.), *Coastal-Offshore Ecosystem Interactions*, Springer-  
 363 Verlag, Berlin, 69–101, 1988.

364 Gueguen, C., Guo, L., Wang, D., Tanaka, N., Hung, C.-C.: Chemical characteristics and origin  
 365 of dissolved organic matter in the Yukon River, *Biogeochemistry*, 77, 139-155, 2006.

366 Hedges, J. I.: Global biogeochemical cycles: progress and problems, *Mar. Chem.*, 39, 67-93,  
 367 1992.

368 Huang, W., and Chen, R. F.: Sources and transformations of chromophoric dissolved organic  
 369 matter in the Neponset River Watershed, *Journal of Geophysical Research: Biogeosciences*,  
 370 114, 2009.

371 Jaffé, R., Boyer, J., Lu, X., Maie, N., Yang, C., Scully, N., and Mock, S.: Source  
 372 characterization of dissolved organic matter in a subtropical mangrove-dominated estuary by  
 373 fluorescence analysis, *Mar. Chem.*, 84, 195-210, 2004.

374 Jeong, K.-S., Kim, D.-K., and Joo, G.-J.: Delayed influence of dam storage and discharge on  
 375 the determination of seasonal proliferations of *Microcystis aeruginosa* and *Stephanodiscus*  
 376 *hantzschii* in a regulated river system of the lower Nakdong River (South Korea), *Water Res.*,  
 377 41(6), 1269-1279.

378 Kim, T.-H., Kim, G., Lee, S.-A., and Dittmar, T.: Extraordinary slow degradation of dissolved  
 379 organic carbon (DOC) in a cold marginal sea, *Sci. Rep.*, 5, 2015.

380 Laane, R.: Conservative behaviour of dissolved organic carbon in the Ems-Dollart estuary and  
 381 the western Wadden Sea, *Neth. J. Sea Res.*, 14, 192-199, 1980.

382 Lang, S. Q., Lilley, M. D., and Hedges, J. I.: A method to measure the isotopic ( $^{13}\text{C}$ )  
 383 composition of dissolved organic carbon using a high temperature combustion instrument, *Mar.*  
 384 *Chem.*, 103, 318-326, 2007.

385 Ludwig, W., Probst, J. L., and Kempe, S.: Predicting the oceanic input of organic carbon by  
 386 continental erosion, *Global Biogeochem. Cycles*, 10, 23-41, 1996.

387 Maie, N., Boyer, J. N., Yang, C., and Jaffé, R.: Spatial, geomorphological, and seasonal  
 388 variability of CDOM in estuaries of the Florida Coastal Everglades, *Hydrobiologia*, 569, 135-  
 389 150, 2006.

390 Mantoura, R., and Woodward, E.: Conservative behaviour of riverine dissolved organic carbon  
 391 in the Severn Estuary: chemical and geochemical implications, *Geochim. Cosmochim. Acta*,  
 392 47, 1293-1309, 1983.

393 Markager, S., Stedmon, C. A., and Søndergaard, M.: Seasonal dynamics and conservative  
 394 mixing of dissolved organic matter in the temperate eutrophic estuary Horsens Fjord, *Estuarine*  
 395 *Coastal Shelf Sci.*, 92, 376-388, 2011.

396 Mayer, L. M., Schick, L. L., and Loder, T. C.: Dissolved protein fluorescence in two Maine  
 397 estuaries, *Mar. Chem.*, 64, 171-179, 1999.

398 Meybeck, M.: Carbon, nitrogen, and phosphorus transport by world rivers, *Am. J. Sci.*, 282,  
 399 401-450, 1982.

400 Moran, M. A., Pomeroy, L. R., Sheppard, E. S., Atkinson, L. P., and Hodson, R. E.: Distribution  
 401 of terrestrially derived dissolved organic matter on the southeastern US continental shelf,  
 402 *Limnol. Oceanogr.*, 36, 1134-1149, 1991.

403 Moyer, R. P., Powell, C. E., Gordon, D. J., Long, J. S., and Bliss, C. M.: Abundance, distribution,  
 404 and fluxes of dissolved organic carbon (DOC) in four small sub-tropical rivers of the Tampa  
 405 Bay Estuary (Florida, USA), *Applied Geochemistry*, 63, 550-562, 2015.

406 Panetta, R. J., Ibrahim, M., and Gélinas, Y.: Coupling a High-Temperature Catalytic Oxidation  
 407 Total Organic Carbon Analyzer to an Isotope Ratio Mass Spectrometer To Measure Natural-  
 408 Abundance  $\delta^{13}\text{C}$ -Dissolved Organic Carbon in Marine and Freshwater Samples, *Anal. Chem.*,  
 409 80, 5232-5239, 2008.

410 Qualls, R. G., Haines, B. L., and Swank, W. T.: Fluxes of dissolved organic nutrients and humic  
 411 substances in a deciduous forest, *Ecology*, 72, 254-266, 1991.

412 Raymond, P. A., and Bauer, J. E.: DOC cycling in a temperate estuary: a mass balance approach  
 413 using natural  $^{14}\text{C}$  and  $^{13}\text{C}$  isotopes, *Limnol. Oceanogr.*, 46, 655-667, 2001.

414 Romera-Castillo, C., Sarmiento, H., Álvarez-Salgado, X. A., Gasol, J. M., and Marrasé, C.: Net  
 415 production and consumption of fluorescent colored dissolved organic matter by natural  
 416 bacterial assemblages growing on marine phytoplankton exudates, *Applied and environmental  
 417 microbiology*, 77, 7490-7498, 2011.

418 Spiker, E.: The Behavior of C-14 and C-13 in Estuarine Water-Effects of Insitu  $\text{CO}_2$  Production  
 419 and Atmospheric Exchange, *Radiocarbon*, 22, 647-654, 1980.

420 Stedmon, C. A., Markager, S., Søndergaard, M., Vang, T., Laubel, A., Borch, N. H., and  
 421 Windelin, A.: Dissolved organic matter (DOM) export to a temperate estuary: seasonal  
 422 variations and implications of land use, *Estuaries and Coasts*, 29, 388-400, 2006.

423 Steinberg, D. K., Nelson, N. B., Carlson, C. A., and Prusak, A. C.: Production of chromophoric  
 424 dissolved organic matter (CDOM) in the open ocean by zooplankton and the colonial  
 425 cyanobacterium *Trichodesmium* spp, *Mar. Ecol. Prog. Ser.*, 267, 45-56, 2004.

426 Vignudelli, S., Santinelli, C., Murru, E., Nannicini, L., and Seritti, A.: Distributions of  
 427 dissolved organic carbon (DOC) and chromophoric dissolved organic matter (CDOM) in  
 428 coastal waters of the northern Tyrrhenian Sea (Italy), *Estuarine Coastal Shelf Sci.*, 60, 133-149,  
 429 2004.

430 Wang, X.-C., Chen, R. F., and Gardner, G. B.: Sources and transport of dissolved and  
 431 particulate organic carbon in the Mississippi River estuary and adjacent coastal waters of the  
 432 northern Gulf of Mexico, *Mar. Chem.*, 89, 241-256, 2004.

433 Zepp, R. G., Sheldon, W. M., and Moran, M. A.: Dissolved organic fluorophores in

434 southeastern US coastal waters: correction method for eliminating Rayleigh and Raman  
435 scattering peaks in excitation–emission matrices, *Mar. Chem.*, 89, 15-36, 2004.

436 Zhang, Y., van Dijk, M. A., Liu, M., Zhu, G., and Qin, B.: The contribution of phytoplankton  
437 degradation to chromophoric dissolved organic matter (CDOM) in eutrophic shallow lakes:  
438 field and experimental evidence, *water research*, 43, 4685-4697, 2009.

439 Zhao, Z., Gonsior, M., Luek, J., Timko, S., Ianiri, H., Hertkorn, N., Schmitt-Kopplin, P., Fang,  
440 X., Zeng, Q., and Jiao, N.: Picocyanobacteria and deep-ocean fluorescent dissolved organic  
441 matter share similar optical properties, *Nature Communications*, 8, 2017.

442

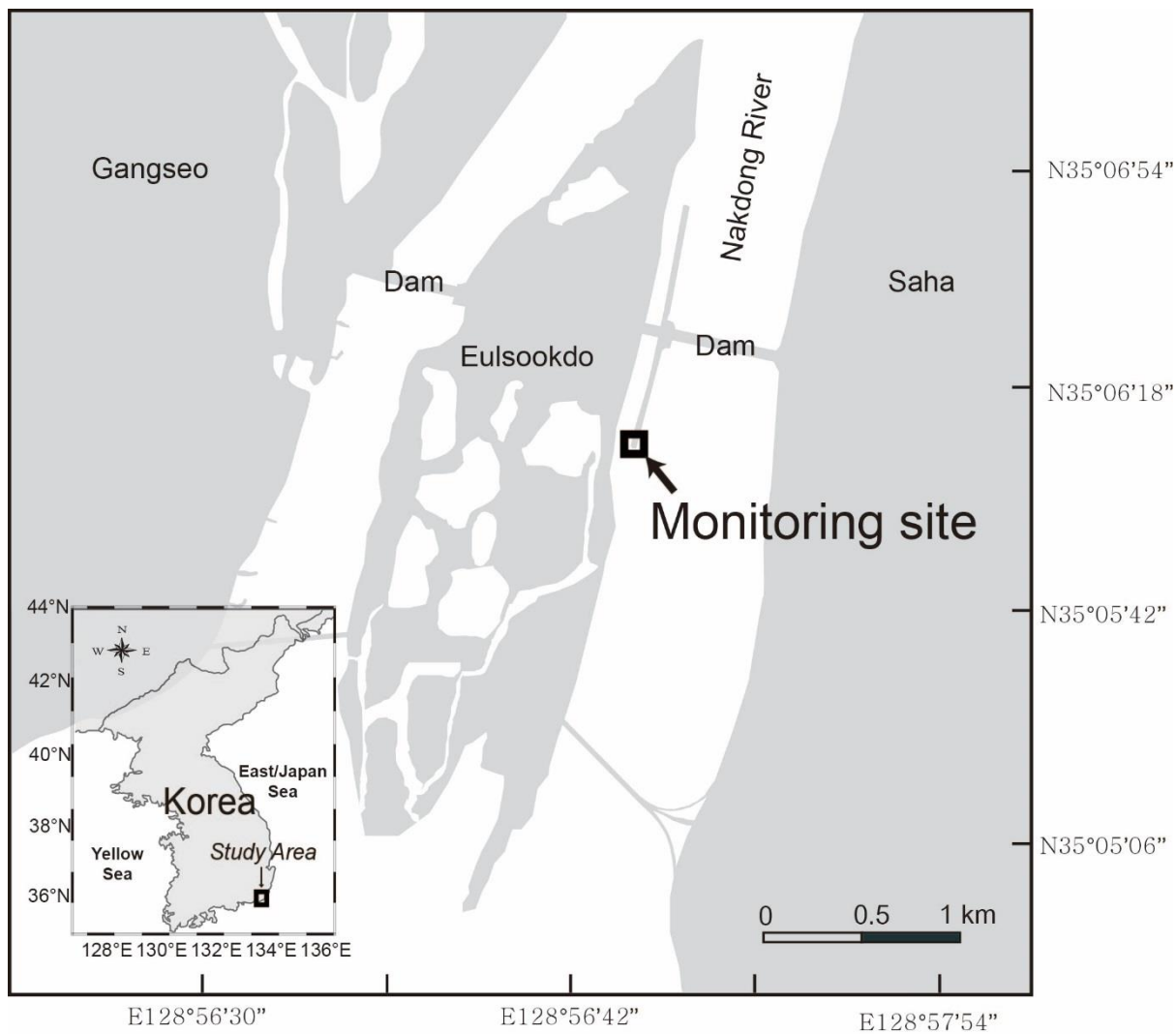


Figure 1. Map of the Nakdong-River Estuary. The square indicates a fixed monitoring site, located 560 m downstream from the dam.

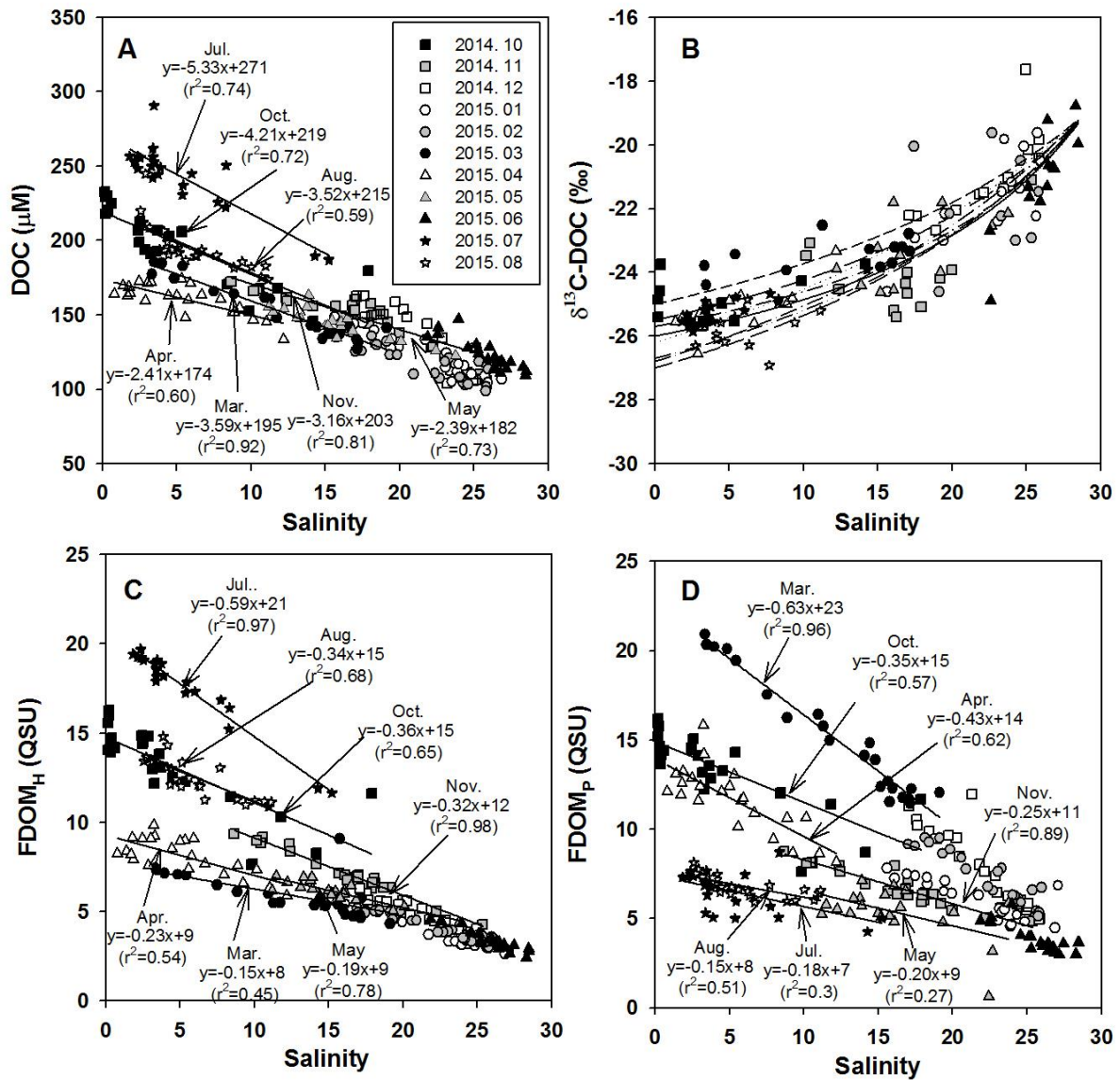
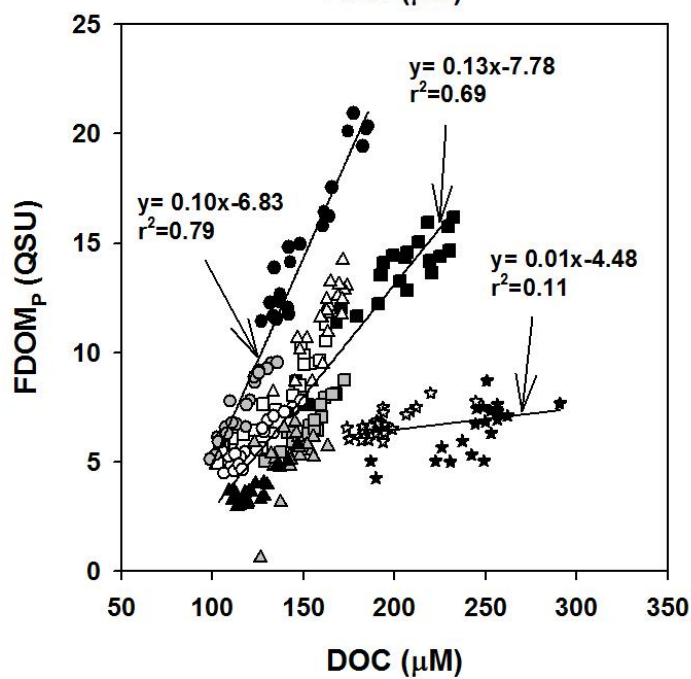
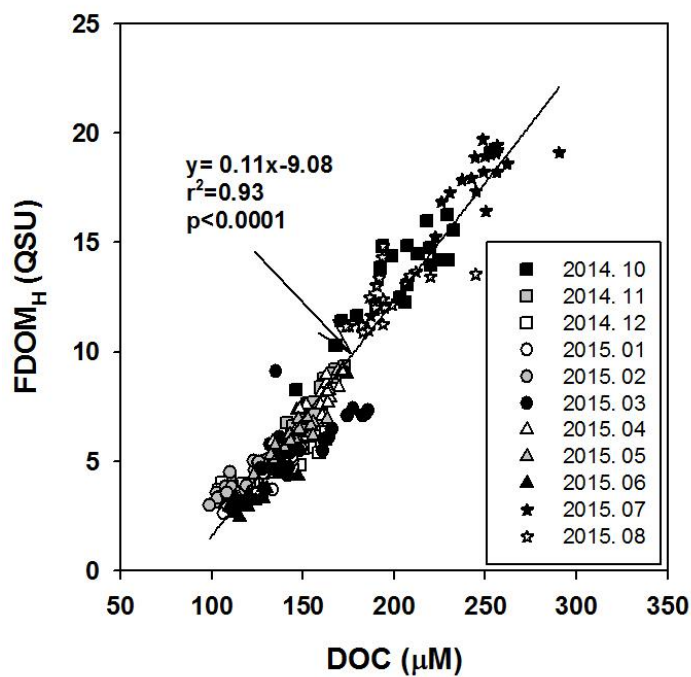


Figure 2. Salinities versus the concentrations of (A) DOC, (B)  $\delta^{13}\text{C-DOC}$ , (C) FDOM<sub>H</sub>, and (D) FDOM<sub>P</sub>. The values for the regression lines are excluded for high-salinity periods (>20), including December, January, February, and June, which have large uncertainties in extrapolation. The solid curve (B) is the average conservative mixing line for the two endmember mixing equation. The dotted lines represent the monthly changes in mixing lines for the different monthly endmember values.



454

455 Figure 3. The plots of the concentrations of DOC versus the concentrations of (A) FDOM<sub>H</sub> and

456 (B) FDOM<sub>P</sub>.

457



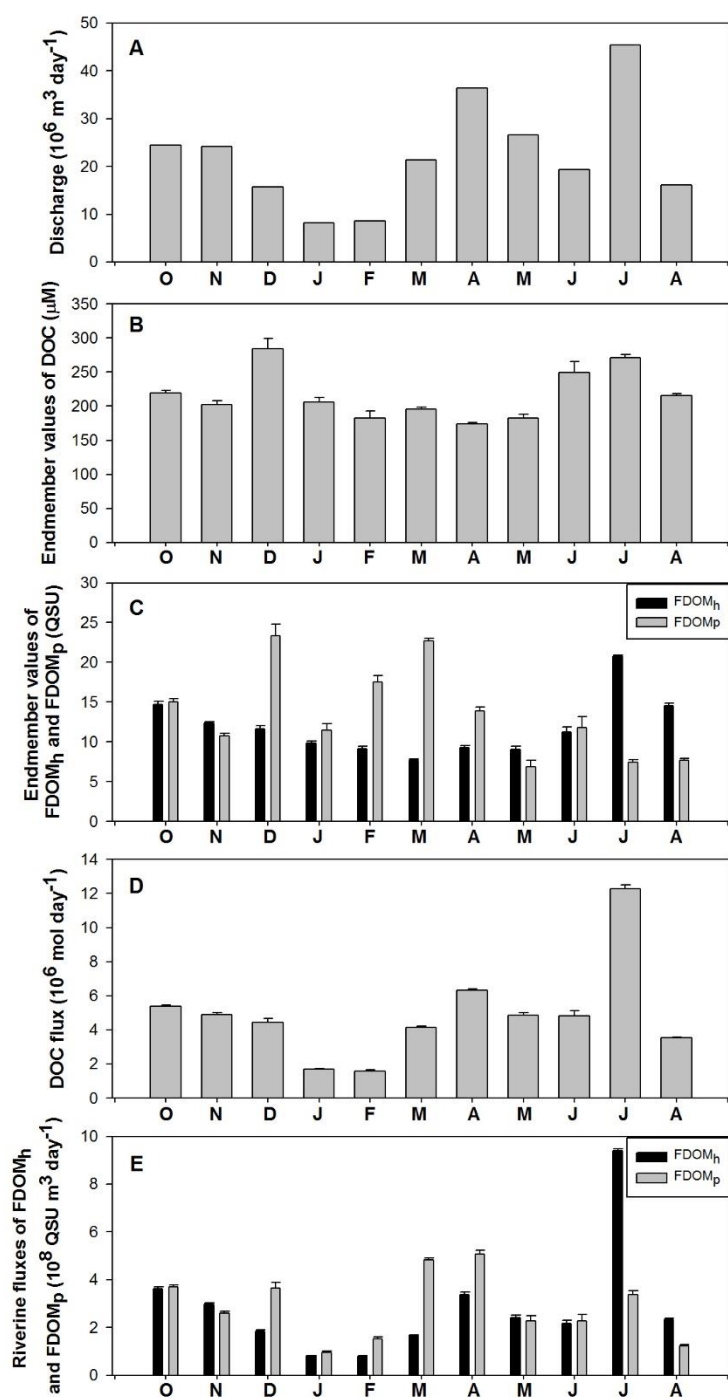


Figure 4. Temporal variations in discharge volumes, the endmember values of DOC, FDOM<sub>H</sub>, and FDOM<sub>P</sub>, and riverine fluxes of DOC, FDOM<sub>H</sub>, and FDOM<sub>P</sub> in the Nakdong-River Estuary from October 2014 to August 2015.